First-principles calculation on the Curie temperature of Gd_3NiSi_2

2009 J. Phys.: Condens. Matter 21 416002

(http://iopscience.iop.org/0953-8984/21/41/416002)

J. Phys.: Condens. Matter **21** (2009) 416002 (6pp) doi:10.1088/0953-8984/21/41/416002

First-principles calculation on the Curie temperature of Gd_3NiSi_2

X B Liu[1] **and Z Altounian**

Center for the Physics of Materials and Department of Physics, McGill University, Rutherford Physics Building, 3600 University Street, Montreal, QC, H3A 2T8, Canada

E-mail: liux@physics.mcgill.ca

Received 23 July 2009, in final form 26 August 2009
Published 23 September 2009
Online at stacks.iop.org/JPhysCM/21/416002

Abstract

The electronic structure and magnetic properties for Gd_3NiSi_2 have been studied theoretically from a first-principles density functional calculation. The energy band structure is calculated in a local spin density approximation (LSDA), and in a LSDA + Hubbard U approach (LSDA + U), respectively. For Gd atoms, in the LSDA + U approximation, seven spin-up 4f bands are fully occupied and situated at the bottom of Si s states, while the spin-down 4f hole levels are completely unoccupied and well above the Fermi level. The calculated magnetic moments for the three Gd sites vary from 7.13 to 7.16 μ_B, leading to a total magnetization of 21.5 μ_B per formula unit including the small induced moments at Ni and Si atoms. The exchange coupling parameters for the nearest Gd–Gd pairs (J_{Gd-Gd}) are 0.16 mRyd, 0.14 mRyd and 0.19 mRyd in the three Gd sub-lattices, respectively. The inter-site distance dependence of J_{Gd-Gd} shows a RKKY-like oscillation. The estimated Curie temperature is about 251 K from the calculated exchange coupling parameters based on the mean-field approximation, in good agreement with the experimental value ($T_C^{exp.} = 215$ K).

(Some figures in this article are in colour only in the electronic version)

1. Introduction

Room temperature magnetic refrigeration, based on the magnetocaloric effect (MCE), has attracted considerable attention because of its energy saving potential and being friendly to the environment [1, 2]. The MCE shows its peak value around the Curie temperature, T_C, for ferromagnetic materials. Generally, the magnetic refrigerant is composed of several MCE materials with different T_C to meet the need of working in a specific range of temperatures. Predicating and tuning T_C is important in developing new MCE materials.

Since the giant magnetocaloric effect (MCE) was discovered in $Gd_5Si_xGe_{4-x}$ [1], increased research attention has been paid to Gd-based compounds. Gd-based compounds are traditionally considered to be ideal local moment systems. It is expected that their exchange coupling could be described by a Heisenberg Hamiltonian so that their finite temperature magnetic properties could be studied. The Heisenberg interatomic exchange parameters are calculated from first principles on the basis of the density functional theory. The most frequently used method is a linear response method suggested by Liechtenstein *et al* [3]. The formula gives an analytical expression for the second derivative of the band energy with respect to the deviations of the atomic moments. Another method is based on the total-energy calculations for a set of different collinear magnetic structures. The calculation could be performed using any standard DFT code, but requires using large magnetic supercells [4].

Although there are many theoretical calculations on the electronic structure of Gd-based compounds (see, for example, [5–14]), only a few publications are on the magnetic exchange interactions [12–14]. Turek *et al* [12] applied a real-space Green function formalism to study the exchange pair interactions between distant neighbors for Gd metal. Mitra *et al* [13] have extracted the exchange coupling parameters using a Heisenberg model by calculating the total-energy differences between the ferromagnetic (FM) and antiferromagnetic (AFM) configurations for Gd-pnictides.

Gd_3NiSi_2 has an orthorhombic, filled-up Hf_3P_2 type structure with a space group of *Pnma* [15]. The compound is a ferromagnet with a Curie temperature, T_C, of 215 K and has a peak value of the isothermal magnetic entropy change

[1] Author to whom any correspondence should be addressed.

of 6.3 J kg^{-1} K^{-1} under a field change of 4.6 T [16]. This compound could be a good candidate as a magnetic refrigerant in the corresponding temperature range.

Up to now, the electronic structure and exchange interaction have not yet been calculated theoretically or investigated experimentally for the Gd_3NiSi_2 compound. We, here, have calculated the electronic structure in the local spin density approximation (LSDA) and LSDA + Hubbard U approximation and derived the magnetic exchange coupling parameters using a linear response method for the orthorhombic Gd_3NiSi_2 compound.

2. Computational methods and crystal structure

In our electronic structure calculations, we apply the linear muffin-tin orbital method within the atomic sphere approximation (LMTO-ASA) [17, 18]. The relativistic effects are treated by solving a scalar relativistic wave equation. Spin–orbit coupling does not affect the overall band structure very much except for some minor details. However, spin-up and spin-down states are then mixed. Therefore, all band structures are calculated without spin–orbit coupling and a single non-self-consistent calculation including spin–orbit coupling is performed to obtain the orbital magnetic moments. The real-space structure constants are generated using a maximum cluster sphere radius of five times the average Wigner–Seitz radius in the compound and the convergence is better than 10^{-5}. The k-space integrations were performed with the tetrahedron method and the charge self-consistency and the exchange coupling parameters were obtained with 637 and 3025 irreducible k-points, respectively. Exchange and correlation effects are treated with LSDA parameterizations given by von Barth and Hedin [19]. The Gd 4f electrons are treated using an LSDA + U method for the exchange–correlation effect [20–22]. In the LSDA + U approach, the screened Coulomb and exchange energy of a chosen set of localized orbitals (here, Gd 4f states) are added to the usual LSDA functional and their orbital independent average is subtracted to avoid double counting. The present implementation follows the rotationally invariant formulation of Liechtenstein *et al* [20]. The fully localized limit (FLL) versions of the LSDA + U double counting was used here because of the highly localized nature of the 4f orbitals. The Coulomb repulsion U describes the extra energy to separate an excited f electron and the resulting f hole over the LDA bandgap while the effective exchange J parameter is an approximation to the Stoner exchange energy. The Coulomb elements can be written in terms of Clebsch–Gordon coefficients and the radial Slater–Coulomb integrals F^k, with $k = 0$, 2, 4 and 6. Generally, only F^0 is strongly screened, whereas F^2, F^4 and F^6 behave as in the free atom. For f electrons, $U = F^0$, and the effective J parameter is given by [22]

$$J = (286F^2 + 195F^4 + 250F^6)/6435. \quad (1)$$

In all the LSDA + U calculations, we use the Hubbard and exchange parameters $U = 6.7$ eV and $J = 0.7$ eV, given by Harmon *et al* [21], for Gd 4f electrons.

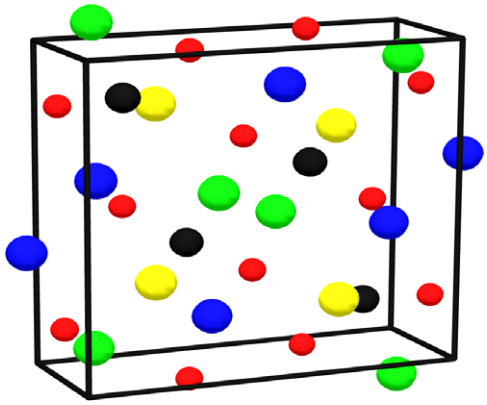

Figure 1. Unit cell for the orthorhombic Gd_3NiSi_2 compound. The large size spheres are for Gd_1 (green/medium gray), Gd_2 (blue/dark gray) and Gd_3 (yellow/light) atoms. The medium (black) and small size (red) spheres stand for Ni and Si atoms, respectively.

The inter-site exchange coupling parameters J_{ij} of the Heisenberg model have been calculated using a linear response method [3]. We adopt a Green's function technique combined with the LMTO method in the calculation [23]. In this approach, exchange interactions are calculated as the response to small-angle fluctuations of the spin orientations. The band structure calculation provides the one-electron Green function. The energy integrals over the occupied part of the valence band were expressed as integrals over an energy variable along a closed path **C** starting and ending at the Fermi energy. The integrals were numerically evaluated using the Gaussian quadrature method.

In the calculations, the experimental lattice constants and atomic positions are used for the Gd_3NiSi_2 compound. Gd_3NiSi_2 crystallizes in orthorhombic structure with a space group of *Pnma* and has lattice constants of $a = 11.398(4)$ Å, $b = 4.155(1)$ Å and $c = 11.310$ Å [15]. The Gd atoms are distributed on three different 4c positions while the Ni and Si atoms occupy one 4c site and two 4c sites, respectively (figure 1).

3. Results and discussion

3.1. Band structure, density of states and magnetic moments

Figure 2 displays the band structure along the main symmetry lines in the LSDA approximation for the Gd_3NiSi_2 compound. The total and partial density of states (DOS) in the LSDA approximation are displayed in figures 3 and 4, respectively. Gd_3NiSi_2 shows a typical metallic behavior in both minority and majority components. The band structure/DOS of Gd_3NiSi_2 could be divided into several regions. The lowest region at about −8 eV have mostly Si s character with some Ni s, p and Gd s, p features mixed in. The next large and sharp DOS peak at −4.5 eV is contributed by the Gd 4f states. Ni 3d and Si 3p states are mainly distributed between the Gd 4f peak and the Fermi level, E_f. On the other hand, Gd 5d states are situated between −4.5 and 10 eV, which are strongly hybridized with Si 3p and Ni 3d energy bands. The sharp peak of minority 4f states is located just above the Fermi level.

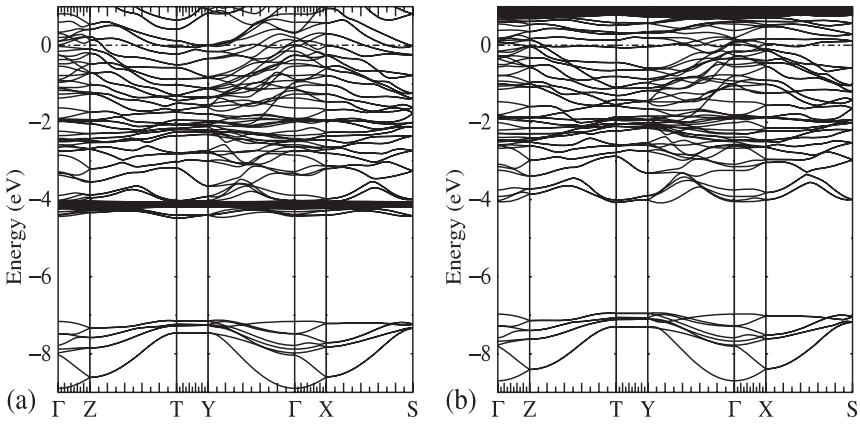

Figure 2. Majority (a) and minority (b) energy band structure along the main symmetry lines, calculated in LSDA for Gd_3NiSi_2. E_f is set to zero on the energy scale.

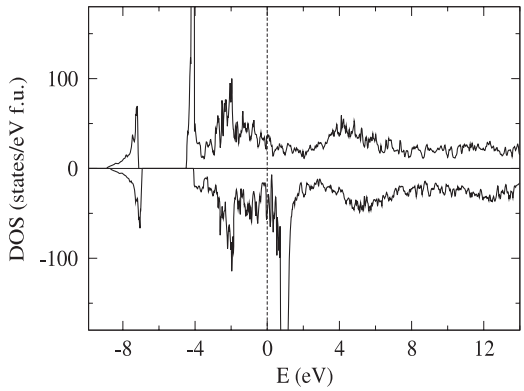

Figure 3. Spin-projected total DOS calculated in LSDA for Gd_3NiSi_2. Majority (minority) spin components are displayed in the positive (negative) y axis. E_f is set to zero on the energy scale.

Table 1. Calculated spin (M_s), orbital (M_o) and total (M_t) atomic magnetic moments (μ_B) of Gd_3NiSi_2 in the LSDA + U approximation.

Atom	M_s	M_o	M_t
Gd_1	7.061	0.066	7.127
Gd_2	7.120	0.036	7.156
Gd_3	7.111	0.053	7.164

Table 2. Effective on-site exchange coupling constants J_0 (mRyd) resolved in atomic orbitals for Gd_3NiSi_2 compound.

Atom	J_0	J_{0s}	J_{0p}	M_{0d}	M_{0f}
Gd_1	2.236	0.069	0.631	1.441	0.095
Gd_2	2.014	−0.060	0.610	1.381	0.084
Gd_3	2.784	0.050	0.963	1.666	0.103

The existence of high 4f DOS around the Fermi level in the LSDA calculation is incorrect and results from the underestimation of the strong on-site Coulomb interaction among the Gd 4f electrons. Here, the LSDA + U method was used to treat the Gd 4f electrons. The LSDA + U band structure and total DOS with LSDA + U approximation is shown in figures 5 and 6. As expected, the majority 4f states are completely occupied by seven electrons and are situated around −8 eV below E_f (just at the bottom of the Si s states) while the minority 4f states are empty and at about 6 eV above E_f. The DOS near E_f is dominated by Gd 5d, Si 3p and Ni 3d states. The empty 4f hole levels are well above E_f and hybridized with Gd 5d states.

Table 1 displays the spin, orbital and total atomic magnetic moments for Gd_3NiSi_2 in LSDA + U approximations. As expected, the orbital moments are very small. The calculated magnetic moments at Gd sites are slightly larger than the Gd 4f value of 7 μ_B due to the small induced Gd 5d moments. Including the small induced moment at Ni (0.08 μ_B) and Si (−0.01 μ_B) sites, the calculated total magnetization per formula unit is of 21.53 μ_B, in excellent agreement with the experimental value (21.58 μ_B per formula unit) given by Tence *et al* [16]. It should be noted that the moments at Gd sites (7.13–7.16 μ_B) is smaller than the calculated moment of Gd (7.74 μ_B) in the Gd pure metal [21]. This results from the state hybridization between Gd 5d states and the states of Si 3p and Ni 3d (figures 4 and 5). In fact, the nearest and next-nearest neighbors of Gd are Ni and Si in this compound, respectively (figure 1).

3.2. Exchange interaction

Exchange interaction is responsible for the magnetic moment formation and the pattern of magnetic ordering [24]. Using the linear response method, we calculate the inter-site exchange coupling constant, J_{ij}, and the on-site effective exchange coupling constant, J_0, which is the sum of the exchange coupling constants of a given magnetic moment with all the other moments within a given cutoff radius R. (Here, $R = 5a$, where a is the lattice constant.) As expected, the main contribution to the magnetic exchange interaction is from the Gd atoms. The value of J_0 at the Gd sites varies from 2.0 to 2.8 mRyd (table 2).

As shown in figure 1, there are three Gd sites in the Gd_3NiSi_2 compound. Figure 7 displays the Gd–Gd inter-site exchange coupling parameters J_{ij} in the three Gd sub-lattices for the Gd_3NiSi_2 compound. As shown in figure 7,

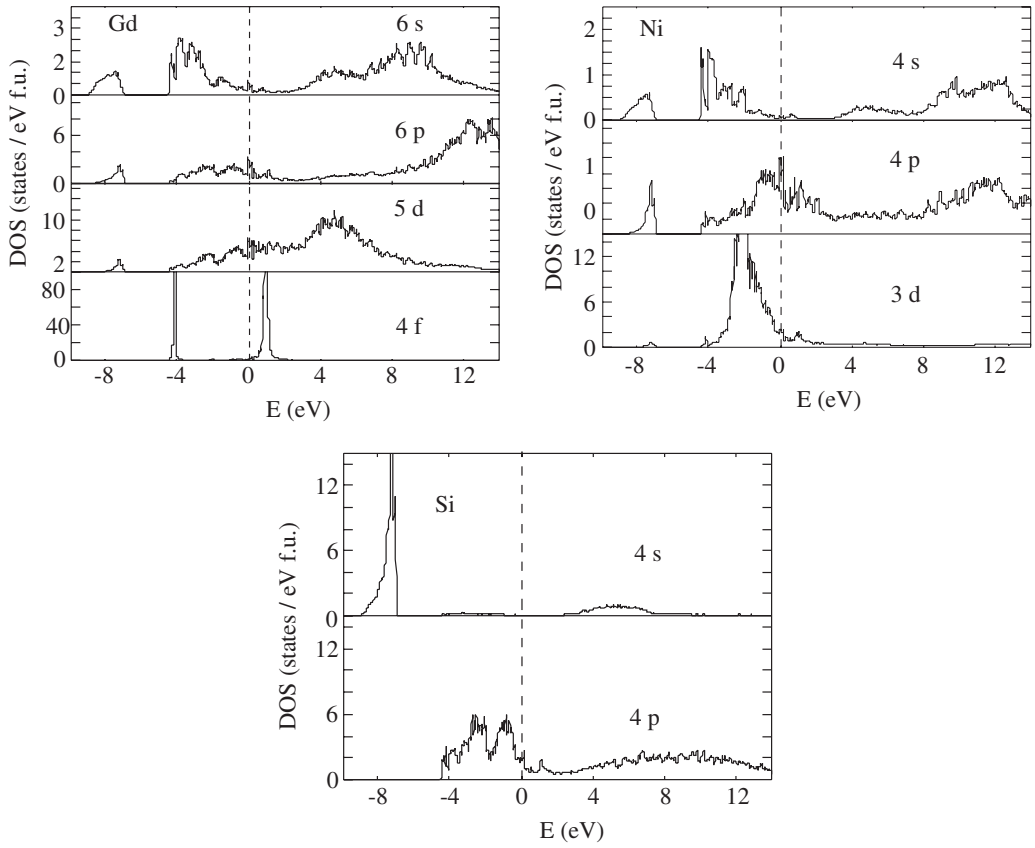

Figure 4. Atomic orbital resolved partial DOS calculated for Gd_3NiSi_2 in LSDA. E_f is set to zero on the energy scale.

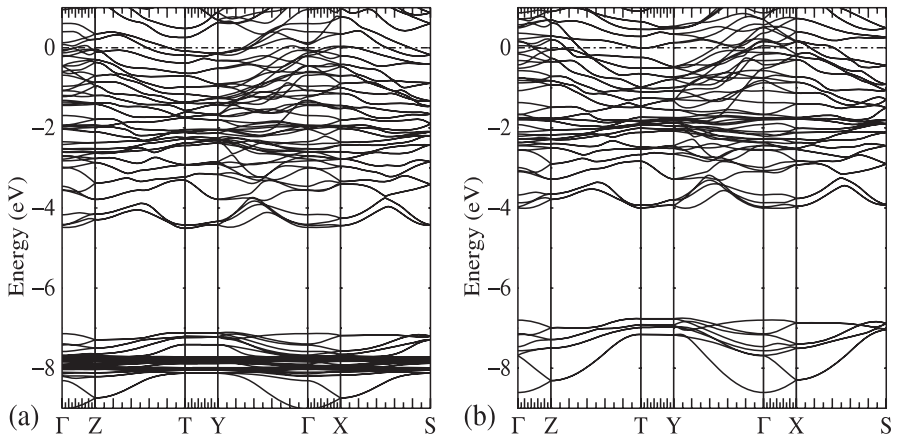

Figure 5. Majority (a) and minority (b) energy band structure along the main symmetry lines, calculated in LSDA + U for Gd_3NiSi_2. E_f is set to zero on the energy scale.

the inter-site Gd–Gd exchange interaction depends on the interatomic distance and the different Gd sub-lattice. The Gd–Gd exchange coupling parameters decrease rapidly with increasing Gd–Gd interatomic distance. The nearest inter-site exchange interaction is the most important to the magnetic ordering. The nearest exchange coupling parameter of Gd–Gd J_{01}^{Gd1} is 0.161 mRyd in the Gd_1 sub-lattice. Similarly, J_{01}^{Gd2} and J_{01}^{Gd3} are 0.144 mRyd and 0.189 mRyd, respectively.

Figure 8 shows the Gd–Gd inter-site exchange coupling parameters, J_{ij}, between different Gd sub-lattices in the Gd_3NiSi_2 compound. Again, the Gd–Gd pair exchange coupling parameters tend to decrease rapidly with increasing interatomic distance. The nearest Gd–Gd exchange coupling parameters between different Gd sub-lattices are clearly larger than those in each single sub-lattice. This could be related to the different near-neighbor environments for the different Gd sites.

Ignoring the difference of Gd at the different sites, the inter-site exchange coupling parameters of Gd–Gd pairs, J_{Gd}, with a pre-factor $(R/a)^3$, as a function of inter-site distance is

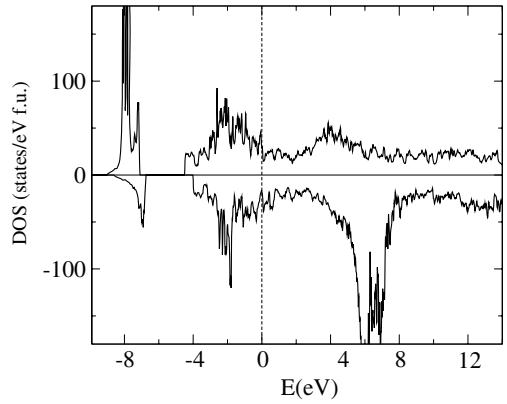

Figure 6. Spin-projected total DOS in the LSDA + U approximation for Gd_3NiSi_2. Majority (minority) spin components are displayed in the positive (negative) y axis. E_f is set to zero on the energy scale.

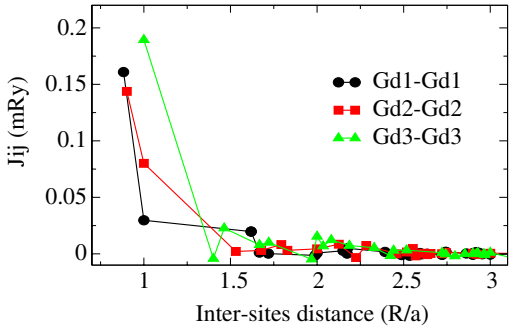

Figure 7. The exchange coupling parameters as a function of the inter-site distance for Gd_1–Gd_1, Gd_2–Gd_2 and Gd_3–Gd_3 pairs in Gd_3NiSi_2. a is the lattice constant.

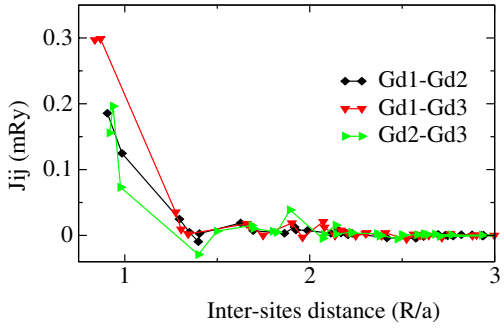

Figure 8. The exchange coupling parameters as a function of the inter-site distance for Gd_1–Gd_2, Gd_1–Gd_3 and Gd_2–Gd_3 pairs in Gd_3NiSi_2. a is the lattice constant.

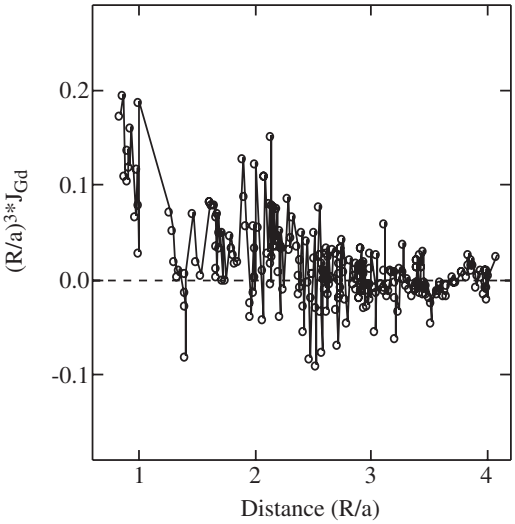

Figure 9. The exchange coupling parameters for Gd–Gd pairs, J_{Gd}, with a pre-factor $(R/a)^3$ as a function of the inter-site distance in Gd_3NiSi_2. a is the lattice constant.

shown in figure 9. The inter-site distance dependence of J_{Gd} shows an exponentially damped Ruderman–Kittel–Kasuya–Yoshida (RKKY)-like oscillation. This conforms to the fact that the RKKY-like exchange interaction dominates in the rare earth metal and compound [25].

In order to gain more insight on the origin of the magnetic exchange interaction, table 2 displays the value of J_0 resolved in atomic orbitals for the Gd_3NiSi_2 compound. The contributions to J_0 at Gd sites are mainly from 5d and 6p electrons, which conforms to the fact that the 5d and 6p DOS states dominate at E_f. The direct contribution of the 4f electron is small (table 2), because their magnetic moments are localized and give no direct interaction with neighbors while they induce a moment on Gd 5d via f–d interaction. These calculation results conform to the general viewpoint that the overlap between the neighboring 4f states is negligible and the 6s, 6p and 5d electrons mediate a RKKY exchange interaction to couple the 4f moments [25].

In the framework of the mean-field approximation (MFA), the Curie temperature T_C for multiple sub-lattices is calculated as the largest eigenvalue of the equation [26, 27]

$$\det(T_{pq} - T\delta_{pq}) = 0 \qquad (2)$$

where p and q are the indices of the nonequivalent magnetic sub-lattices and $T_{pq} = 2J^0_{p,q}/3k_B$. $J^0_{pq} = \sum_j J_{p0,qj}$, where $J_{p0,qj}$ is the exchange coupling between the zeroth atom at sub-lattice p and the jth atom at sub-lattice q.

As mentioned above, there are three Gd sites, one Ni site and two Si sites in the compound. In our case, the Gd–Gd exchange interaction dominates in the magnetic ordering. Ignoring the contribution of Ni and Si sites to the magnetic ordering, there are three magnetic sub-lattices. The effective exchanging coupling constants for the three Gd sub-lattices are $J^0_{Gd1,Gd1} = 0.488$ mRyd, $J^0_{Gd2,Gd2} = 0.552$ mRyd, $J^0_{Gd3,Gd3} = 0.607$ mRyd, $J^0_{Gd1,Gd2} = 0.486$ mRyd, $J^0_{Gd1,Gd3} = 1.156$ mRyd and $J^0_{Gd2,Gd3} = 0.883$ mRyd. Using equation (2), the derived Curie temperature is 251 K, in good agreement with the experimental value of Gd_3NiSi_2 ($T_C = 215$ K), considering the MFA Curie temperature is generally overestimated by 15% or so [23]. The over-estimation of the MFA T_C could be improved by a Monte Carlo simulation, which can, in principle, provide a more accurate estimation of T_C for the given Hamiltonian.

4. Conclusion

In summary, the Coulomb repulsion U strongly influences the electronic structure of the Gd_3NiSi_2 compound. For Gd atoms,

seven spin-up 4f bands are fully occupied and situated at the bottom of the Si s state, while the 4f hole levels are completely unoccupied and well above the Fermi level in the LSDA + U approximation. Gd_3NiSi_2 shows a typical metallic behavior in both minority and majority components. The calculated magnetic moments for the three Gd sites vary from 7.13 to 7.16 μ_B, leading to a total magnetization of 21.5 μ_B per formula unit including the small induced moments at Ni and Si atoms. The exchange coupling parameters for the nearest Gd–Gd pairs are 0.16 mRyd, 0.14 mRyd and 0.19 mRyd in the three Gd sub-lattices, respectively. The estimated Curie temperature is 251 K from the calculated exchange coupling parameters in the MFA approximation, comparable with the experimental value ($T_C^{exp.} = 215$ K).

Acknowledgments

This work was supported by the Natural and Engineering Research Council of Canada and Fonds pour la Formation de Chercheurs et l'Aide a la Recherche, Quebec.

References

[1] Gschneidner K A Jr, Pecharsky V K and Tsokol A O 2005 *Rep. Prog. Phys.* **68** 1479
[2] Brück E 2005 *J. Phys. D: Appl. Phys.* **38** R381
[3] Lichtenstein A I, Katsnelson M I, Antropov V P and Gubanov V A 1987 *J. Magn. Magn. Mater.* **67** 65
[4] Zhou Y M, Geng W T and Wang D S 1998 *Phys. Rev.* B **57** 5029
[5] Samolyuk G D and Antropov V P 2002 *J. Appl. Phys.* **91** 8540
[6] Harmon B N and Antonov V N 2002 *J. Appl. Phys.* **91** 9815
[7] Paudyal D, Pecharsky V K, Gschneidner K A Jr and Harmon B N 2006 *Phys. Rev.* B **73** 144406
[8] Altounian Z and Liu X B 2007 *J. Appl. Phys.* **101** 09D507
[9] Chantis A N, van Schilfgaarde M and Kotani T 2007 *Phys. Rev.* B **76** 165126
[10] Larson P, Lambrecht W R L, Chantis A and van Schilfgaarde M 2007 *Phys. Rev.* B **75** 045114
[11] Nordstrom L and Mavromaras A 2000 *Europhys. Lett.* **49** 775
[12] Turek I, Kudrnovsky J, Bihlmayer G and Blugel S 2003 *J. Phys.: Condens. Matter* **15** 2771
[13] Mitra C and Lambrecht W R L 2008 *Phys. Rev.* B **78** 134421
[14] Isnard O, Kuzmin M D, Richter M, Loewenhaupt M and Bewley R 2008 *J. Appl. Phys.* **104** 013922
[15] Klepp K and Parthe E 1981 *Acta Crystallogr.* B **37** 1500
[16] Tence S, Gorsse S, Gaudin B and Chevalier B 2009 *Intermetallics* **17** 115
[17] Andersen O K 1975 *Phys. Rev.* B **12** 3060
[18] Andersen O K and Jepsen O 1984 *Phys. Rev. Lett.* **53** 2571
[19] von Barth U and Hedin L 1972 *J. Phys. C: Solid State Phys.* **5** 1629
[20] Anisimov V I, Zaanen J and Andersen O K 1991 *Phys. Rev.* B **44** 943
[21] Harmon B N, Antropov V P, Lichtenstein A I, Solovyev I V and Anisimov V I 1995 *J. Phys. Chem. Solids* **56** 1521
[22] van der Marel D and Sawatzky G A 1988 *Phys. Rev.* B **37** 10674
[23] van Schilfgaarde M and Antropov V P 1999 *J. Appl. Phys.* **85** 4827
[24] Kübler J 2000 *Theory of Itinerant Electron Magnetism* (New York: Oxford University Press)
[25] Kittel C 1976 *Introduction to Solid State Physics* 5th edn (New York: Wiley)
[26] Aharoni A 1996 *Introduction to the Theory of Ferromagnetism* (New York: Oxford University Press)
[27] Kurtulus Y, Dronskowski R, Samolyuk G D and Antropov V P 2005 *Phys. Rev.* B **71** 014425